J. Mater. Environ. Sci. 7 (9) (2016) 3068-3075
ISSN : 2028-2508
CODEN: JMESCN

Bioinspired eco-friendly synthesis of ZrO_2 nanoparticles

I. Uddin[1, 2, *], A. Ahmad[1]

[1]*Division of Biochemical Sciences, National Chemical Laboratory, Pune, India.*
[2]*Nanotechnology Innovation Centre, Department of Chemistry, Rhodes University, Grahamstown, South Africa.*

Received 09 Aug 2015, Revised 20 Jun 2016, Accepted 30 Jun 2016
**Corresponding author. E-mail: usmani.imran@gmail.com ; Tel: (+918445503428)*

Abstract
Here we report the extracellular biosynthesis of zirconia (ZrO_2) nanoparticles under ambient conditions by challenging the fungus *Humicola* sp. with potassium hexafluorozirconate (K_2ZrF_6) as a precursor. Transmission electron micrograph (TEM) showed that nanoparticles are quasi-spherical in shape with an average particle size of 13 nm. The structural investigation was done using selected area electron diffraction (SAED) and powder XRD which show that the nanoparticles are perfectly crystalline with an orthorhombic structure. XPS and FTIR analysis explained the presence of proteins on the nanoparticles surfaces.

Keywords: Zirconia, Biosynthesis, Fungus, Nanoparticles, Characterization

Introduction
Metal oxide nanoparticles (TiO_2, SiO_2, Fe_3O_4, Al_2O_3, ZnO, etc.) exhibit unique physical and chemical properties due to their limited size and high density of edge surface sites [1-7]. These nanoparticles play a prime role in many technologies and globally constitute an exceptionally large volume industry. At nanoscale dimensions, the properties of these nano oxides change dramatically which make them suitable for potentially important applications. Among the transition-metal oxide, zirconia (ZrO_2), owing to its specific properties, carries significant importance from a technological point of view and is widely used in solar cells [8], catalysis [9], gate dielectrics [10], bone implants [11], oxygen sensors [12] and fuel cell electrolytes [13] etc. Many different methods for the synthesis of ZrO_2 nanoparticles are described in the literature, such as hydrothermal synthesis [14], sol-gel process [15], spray pyrolysis [16] and emulsion precipitation [17]. These wet-chemical methods are multi-step techniques and use harsh experimental conditions like high temperatures and pressure. An alternative environmentally benign bottom-up biosynthetic approach using microbes is being proposed in this report. From last few years, green bottom-up approaches using microorganisms have been successfully applied for the synthesis of nanocrystals of metal and metal oxides [18-23].
Biosynthesis of nanoparticles has always been of great interest as an alternate to energy-intensive chemical methods [24-25].These biosynthesized nonmaterial surfaces are inherently capped by proteins and other biomolecules which provide the surface passivation along with prevention from agglomeration and stability of suspension in the aqueous medium.These eco-friendly processes are carried out at ambient conditions of temperature and pressure in the absence of harsh chemicals. Here, we report the synthesis of ZrO_2 nanoparticles using fungus *Humicola* sp.

2. Materials and methods
Materials
Potassium hexafluorozirconate (K_2ZrF_6) guaranteed reagent (GR) grade was purchased from Aldrich. Malt extract powder, yeast extract powder, glucose and peptone were obtained from Himedia, India. All the chemicals were used as received.

Experimental

The fungus, *Humicola* sp. was maintained on MGYP (malt extract, glucose, yeast extract, and peptone) agar slants. Stock cultures were maintained by subculturing at monthly intervals. After growing the fungus at pH 9 and 50°C for 96 hours, the slants were preserved at 15°C. From an actively growing stock culture, subcultures were made on fresh slants and after 96 hours of incubation at pH 9 and 50 °C were used as the starting material for fermentation experiments. For the synthesis of ZrO_2 nanoparticles, the fungus was grown in 250 mL Erlenmeyer flasks containing 100 mL of MGYP medium which is composed of malt extract (0.3%), glucose (1%), yeast extract (0.3%) and peptone (0.5%). Sterile 10% sodium carbonate was used to adjust the pH of the medium to 9. After the pH of the medium was adjusted, the culture was grown with continuous shaking on a rotary shaker (200 rpm) at 50°C for 96 hours. After 96 hours of fermentation, mycelial mass was separated from the culture broth by centrifugation (5000 rpm) at 20°C for 20 minutes and washed thrice with sterile distilled water under sterile conditions.

For the extracellular synthesis of ZrO_2 nanoparticles, the harvested mycelial mass (20 grams of wet mycelia) was resuspended in 100 mL of 10^{-3} M of an aqueous solution of K_2ZrF_6 in 250 mL Erlenmeyer flasks at pH 9. The whole mixture was incubated on a shaker at 50°C (200 rpm). The reaction was carried out for 96 hours and fungal biomass was separated by filter paper to separate the biomass and filtrate under sterile conditions. The biotransformation was routinely monitored at different time intervals. To remove the unbound protein and unreacted precursor, the filtrate was centrifuged three times at 15,000 rpm for 30 minutes while resuspending the precipitate in de-ionized water each time. Further synthesis of nanoparticles was monitored by different characterization techniques.

Characterizations

The size and shape analysis of ZrO_2 nanoparticles was done on a Joel model 1200EX TEM operated at a voltage of 120 KV. For this purpose, the samples were prepared by drop-coating the particles suspended in aqueous medium on carbon coated copper grids. The selected area electron diffraction (SAED) analysis was performed on the same grids. Powder XRD patterns were recorded using Philips X'PERT PRO instrument equipped with X'celerator, a fast solid-state detector on samples drop-coated on a glass substrate. The sample was scanned using X'celerator with a total number of 121 active channels. Iron-filtered Cu Kα radiation (λ=1.5406 Å) was used. XRD patterns were recorded in the 2θ range of 20°-70° with a step size of 0.02° and a time of 5 seconds per step. It is XPS of the samples cast on the Si substrate was carried-out on a VG MicroTech ESCA 3000 instrument. The background of the core level spectra was corrected using the Shirley algorithm, and the chemically distinct species were resolved using a nonlinear least squares curve fitting procedure. FTIR spectroscopy measurement on as prepared ZrO_2 nanocrystals powder taken in KBr pellet was carried out using a Perkin–Elmer Spectrum One instrument. The spectrometer was operated in the diffuse reflectance mode at a resolution of 2 cm^{-1}. To obtain good signal to noise ratio, 128 scans of the film were taken in the range, 450 - 4000 cm^{-1}. UV-Visible spectroscopy measurements were carried out on Jasco dual-beam spectrophotometer (model V-570) operated at a resolution of 1nm.

3. Results and discussion

To probe the morphology of these ZrO_2 nanoparticles, a detailed electron microscopy study was performed on the as-synthesized nanoparticles; Figure (1a) showed that the ZrO_2 nanoparticles formed are irregular in shape with an overall quasi-spherical morphology). Figure (1b) shows the particle size distribution of ZrO_2 nanoparticles which reveals that the average particle size of ZrO_2 nanoparticles is about 11 nm These nanoparticles appear to be well separated from each other since they are stabilized by the extracellular proteins/biomolecules present on the surface, that are responsible for synthesis as well as capping of nanoparticles [26]. To better investigate the crystallinity of particle, the SAED image of as-synthesized ZrO_2 nanoparticles were acquired after approximately 96 hours of reaction. The Scherrer ring pattern characteristic of ZrO_2 is clearly observed showing that the structures seen in TEM are nanocrystalline in nature. In figure (1c), the SAED pattern of ZrO_2 is presented which shows a spot pattern confirming the crystallinity of the as-

synthesized protein coated nanoparticles. These spot patterns correspond to the {200} and {111} crystal planes, which matches well with the reported values [27].

To better investigate crystallinity at single particle level, high resolution transmission electron microscopy was employed. Figures 1(d) show the HR-TEM image of as-synthesized ZrO_2 nanoparticles, which show very good crystallinity with very few defects. The extent of single crystallinity observed here in biologically synthesized nanoparticles (fabricated in ambient conditions) is quite remarkable. The lattice planes {111} with a spacing of <2.839 Å> could be observed for the as-synthesized sample.

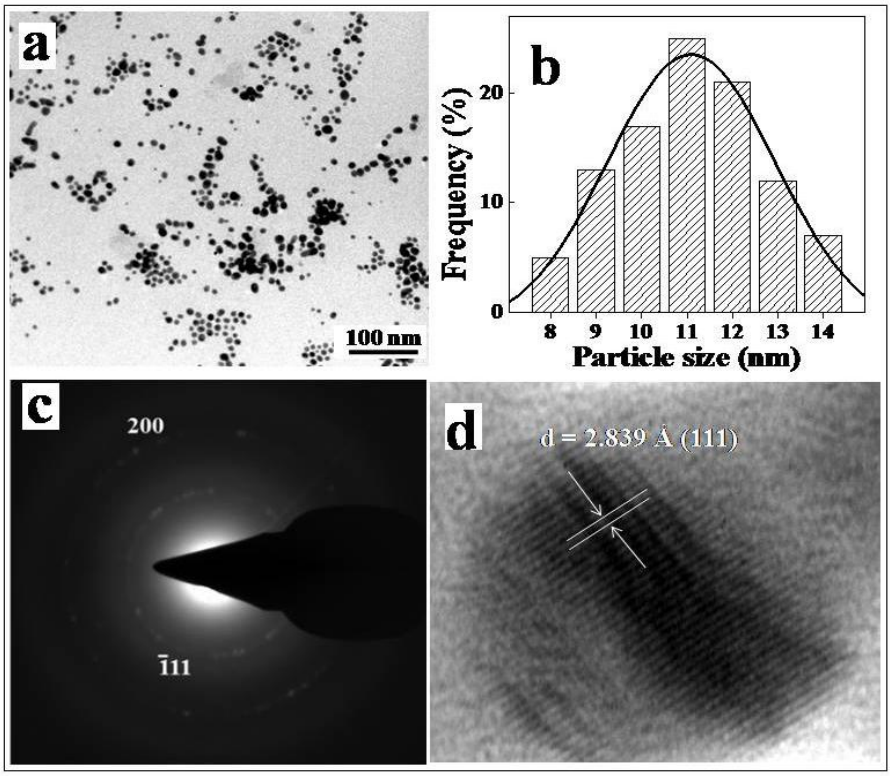

Figure 1: (a) Transmission electron micrograph (TEM) of ZrO_2 nanoparticles; (b) Particle size distribution of ZrO_2 nanoparticles determined from TEM micrographs. The solid line is a Gaussian fit to the histogram (c) SAED pattern recorded from extracellular ZrO_2 nanoparticles shown in TEM micrograph; and (d) HR-TEM image of an individual ZrO_2 nanoparticle.

To further verify the crystallinity of ZrO_2 nanoparticles, X-ray diffraction patterns were recorded from a drop cast film of as-synthesized ZrO_2 nanoparticles on a glass substrate. This shows intense peaks corresponding to the planes, { $\bar{1}$11}, {111}, {200}, and {022}. The peak position and 2θ values agree with those reported for ZrO_2 nanoparticles (figure 2). As-prepared ZrO_2 nanoparticles show well-defined Bragg's reflections indicating that the particles are crystalline in nature. Almost all peaks in the pattern recorded could be indexed to orthorhombic ZrO_2, which is close to the one reported in the literature [27, 28].

The presence of ZrO_2 nanoparticles was also confirmed by analyzing the sample by XPS as shown in figure 3. The results showed the presence of C, N, O and Zr as the prominent elements. The chemical analysis of ZrO_2 nanoparticles was carried out by X-ray photoelectron spectroscopy (XPS) of the samples after 96 hours of the reaction between fungus *Humicola* sp. and K_2ZrF_6. The C 1s, N 1s, O 1s, and Zr 3d core level spectra were recorded with an overall resolution of ~1 eV. The core level binding energies (BEs) were aligned with respect to the C 1s binding energy (BE) of 285 eV. As we know very well, XPS is a highly surface sensitive technique and the protein present on the surface of nanoparticles can easily be identified using XPS. In order

to prove that the ZrO_2 nanoparticles are capped with protein, C1s, N1s, and O1s XPS analysis was done for the biogenic ZrO_2 nanoparticles.

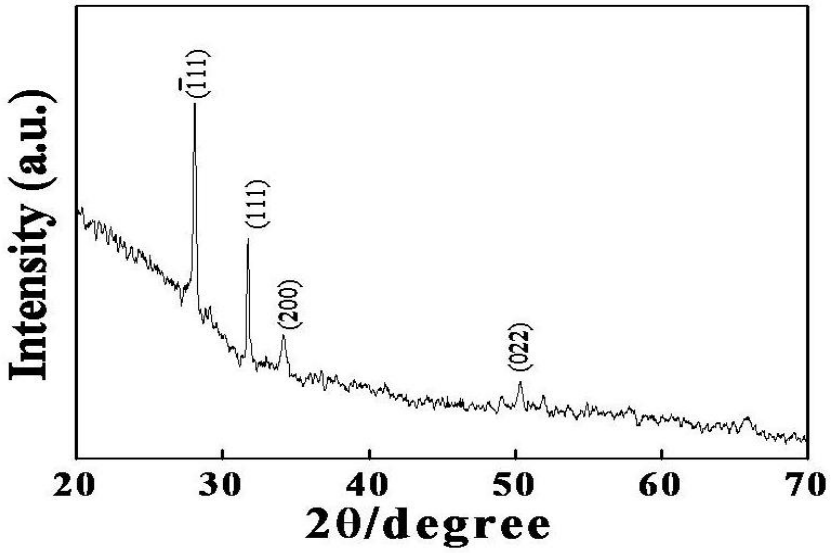

Figure 2: Powder XRD-pattern of drop-cast films of ZrO_2 nanoparticles on a glass substrate. The Braggs reflections arising from the film are indexed with the respective crystal planes.

Figure 3A shows that the C 1s core level spectrum could be decomposed into three chemically distinct components centred at 283.12 eV, 285.16 eV, and 287.62 eV. The deconvoluted low binding energy peak at 283.12 eV is attributed to the presence of aromatic carbon present in amino acids derived from proteins bound to the surface of ZrO_2 nanoparticles [29].

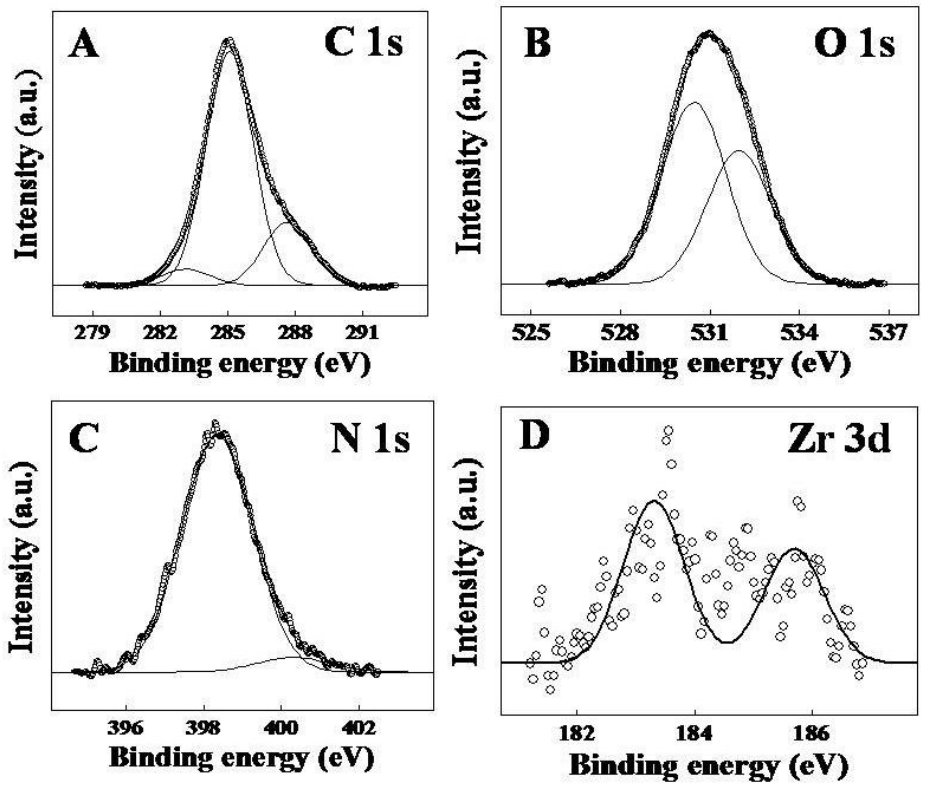

Figure 3: XPS spectra of biosynthesized ZrO_2 nanoparticles; The core level spectra is recorded from C 1s (A), O 1s (B), N 1s (C) and Zr 3d (D). The raw data is shown in the form of symbols while the chemically resolved components are shown as solid lines

The high binding energy peak at 287.62 eV is attributed to electron emission from the carbon of carbonyl groups present in proteins bound to the nanoparticles surface [30]. The C 1s component centred at 285.16 eV is due to electron emission from adventitious carbon present in the sample. The peak in figure 3B corresponds to the chemically distinct core level peak of O 1s. The O 1s spectrum could be resolved into two chemically distinct components with binding energies, 530.32 eV and 531.81 eV. The O 1s component present at lower binding energy at 530.32 can be assigned to the lattice oxygen of the as-prepared ZrO_2 nanoparticles. Beside this, the peak in figure 3B corresponds to the chemically distinct O 1s core level with a binding energy of about 531.81 eV. This may be attributed to the mixed contributions from surface hydroxyl groups (-OH), and C=O group present in capping proteins present on the surface of as-synthesized ZrO_2 nanoparticles [31]. Furthermore, figure 3C shows the N 1s core level spectra that could be fitted into two chemically distinct components centring at 398.48 eV and 400.18 eV. The lower binding energy component could be assigned to free N_2 while higher binding energy component can be attributed to values reported for –NH amide linkage in the capping proteins [32]. Hence, from the above observation in XPS data, it can easily be concluded that nanoparticles are capped with protein, and the growth of oxide nanoparticle is restricted at nanometer scale due to surface bound protein which acts as a capping agent and further stabilizes the oxide nanoparticle in nanometer regime. Figure 3D shows the Zr 3d spectrum of as-synthesized ZrO_2 nanoparticles resolved into two peaks with binding energies of 183.31 and 185.72 eV, attributed to Zr $3d_{5/2}$ and Zr $3d_{3/2}$ peaks respectively in zirconia ion which further conforms to the one reported in the literature [33].
Figure 4A & B presents the comparison of Fourier transform infrared (FTIR) spectra acquired from two different regions of the precursor K_2ZrF_6, without calcination (as-synthesized) and calcined ZrO_2 nanoparticles taken in KBr pellets. It can be noticed that after calcination, the absorption peaks are more prominent. In figure 4A, both without calcination (curve 2) and calcined (curve 3) nanoparticles showed the

presence of a prominent absorption peak around 613 and 819 cm^{-1} due to excitation of the Zr–O–Zr stretching and bending mode vibration respectively which is absent in the spectrum of pure K_2ZrF_6 (figure. 4A, curve 1) [34]. In figure 4B, two absorption bands around 1655 and 1540 cm^{-1} are present in without calcination ZrO_2 sample which might be due to the amide I and II bands that arise due to the carbonyl stretch and –N-H stretch vibrations respectively in the amide linkages of the proteins [35]. Calcination of ZrO_2 nanoparticles at 400ºC for three hours resulted in the denaturation of proteins as is evident from the disappearance of bands around 1655 and 1540 cm^{-1} for the calcined ZrO_2 sample [36]. This shows the removal of protein from the surface of zirconia (ZrO_2) nanoparticles after calcination which again offers evidence that the nanoparticles are capped with protein and restricts its growth during its synthesis. This is the reason why nanoparticles synthesized by biosynthetic methods are much smaller in size.

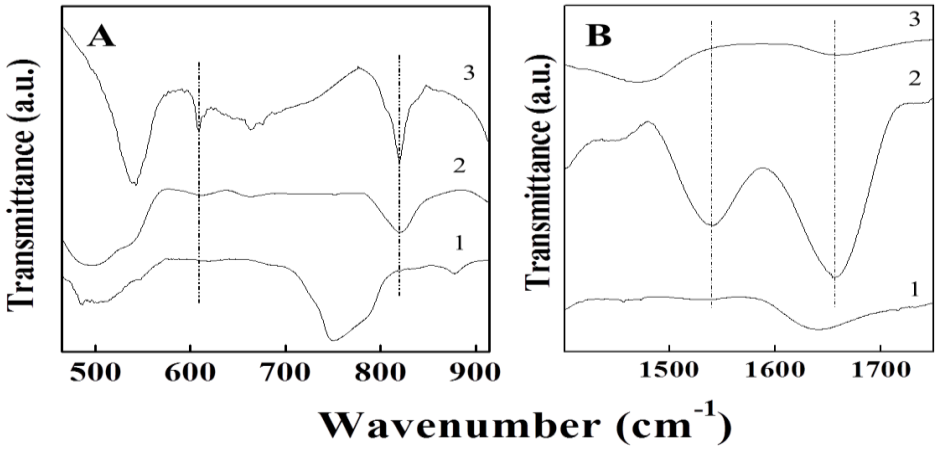

Figure 4: (A) FTIR spectra recorded from powder of K_2ZrF_6 (curve 1); ZrO_2 nanoparticles synthesized using fungus *Humicola* sp. before (curve 2) and after calcination at 400°C for 3 hours (curve 3); (B) Enlarged view of the FTIR spectra shown in the region of the protein amide bands.

An attempt has been made to capture the formation of ZrO_2 nanoparticles by comparing the UV-Visible spectra of the precursors used for the biosynthesis (figure 5) i.e. K_2ZrF_6 (curve 1), with biosynthesized ZrO_2 nanoparticles after 96 hours (curve 2) of reaction. The precursor does not show any significant absorption in the entire range of measurement. However, after the reaction with the fungal biomass for 96 hours, a significant absorption in curve 2 with two broad shoulders appearing, first at ca. 270 nm and later in the range of 310 to 350 nm was observed. The appearance of absorption edge at ca. 270 nm can be assigned to the aromatic amino acids such as tryptophan and tyrosine present in the protein, which is secreted in the broth by the fungus, *Humicola* sp. [37]. We believe that some of the other biomolecules are also responsible for converting ZrF_6^+ ions into stable ZrO_2 nanoparticles. The UV-Visible spectroscopic analysis reveals the presence of broad shoulder in the range from 310 to 350 nm that corresponds to an excitonic transition in ZrO_2 nanocrystallites [38]. There is absence of an absorption edge due to the formation of particles of different sizes.

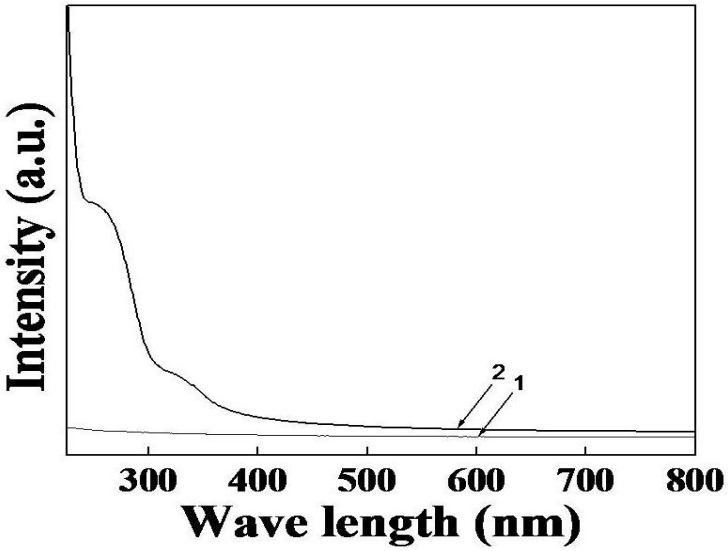

Figure 5: UV-Visible electronic absorption spectra (1) Precursor (K_2ZrF_6); (2) as-synthesized ZrO_2 nanoparticles after 96 hours of reaction.

Conclusion

In conclusion, nanocrystalline water dispersible ZrO_2 nanoparticles were synthesized by bottom-up approach under ambient conditions using fungus *Humicola* sp. and K_2ZrF_6 as the precursor salt. It is also clear that the extracellular proteins secreted by the microorganism play a crucial role in the reduction of the metal ions, defining the morphology and stability of the nanoparticles formed. Hence, these studies suggest that biosynthesis approach is a simple, ecofriendly and efficient process for the synthesis of metal oxide nanoparticles.

Acknowledgements-Imran Uddin thanks the Council of Scientific and Industrial Research (CSIR), New Delhi for Senior Research Fellowship. The authors thank Centre for Materials Characterization (CMC), NCL, Pune, for assistance in TEM, XRD and XPS measurements.

References

1. Yin Z. F., Wu L., Yang H. G., Su Y. H., *Phys Chem Chem Phys*., 15 (2013) 4844.
2. Wang X., Zhang R., Wu C., Dai Y., Song M., Gutmann S., Gao F., Lv G., Li J., Li, X., Guan Z., Fu D., Chen, B., *J Biomed Mater Res A*., 80 (2007) 852.
3. Khan S., Uddin I., Moeez S., Ahmad A., *PLoS ONE*., 9 (2014) e107597.
4. Sridhara V., Satapathy L. N., *Nanoscale Res Lett*., 6 (2011) 456.
5. Uddin I., Venkatachalam S., Mukhopadhyay A., Usmani, M. A., *Current Pharmaceutical Design*., 22 (2016) 1472.
6. Rezaee, A., Soltani, R. D. C., Khataee, A. R., Godini, H., *J. Mater. Environ. Sci.* 3 (2012) 955.
7. Barhon, Z., Saffaj, N., Albizane, A., Azzi, M., Mamouni, R., Haddad, M. E., *J. Mater. Environ. Sci.* 3 (2012) 879.
8. Su Y. H., Lai, Y. S., *Int. J. Energy Res.* 38 (2014) 436.
9. Monopoli A., Calo V., Ciminale F., Cotugno P., Mangone A., Giannossa L. C., Azzone, P., Cioffi N., *Molecules*.15(2010) 4511.
10. Ortiz R. P., Facchetti A., Marks T. J., *Chem. Rev.* 110 (2010) 205.
11. Gillani R., Ercan B., Qiao A., Webster, T. J., *Int J Nanomedicine*. 5 (2010) 1.

12. Ramamoorthy R., Dutta P. K., Akbar S. A., *J Mater Sci* 38 (2003) 4271.
13. Shim J. H., Chao C. C., Huang H., Prinz F. B., *Chem. Mater*. 19 (2007) 3850.
14. Taguchi M., Takami S., Adschiri, T., Nakane, T., Satoa K., Nakaa T., *Cryst Eng Comm*. 14 (2012) 2117.
15. Mahmood Q., Afzal A., Siddiqi H. M., Habib A., *J Sol Gel Sci Technol*., 67 (2013) 670.
16. Song Y. L., Tsai S. C., Chen C. Y., Tseng T. K., Tsai C. S., Chen J. W., Yao Y. D., *J. Am. Ceram. Soc*., 87 (2004)1864.
17. Shi J., Henk Verweij H., *Langmuir* 21 (2005) 5570.
18. Ansary A. A., Uddin I., Khan S. A., *Asian J Phy*., 6 (2014) 1041.
19. Singh A. V., Patil R., Anand A., Milani P., Gade W. N., *Current Nanoscience*., 6 (2015) 365.
20. Singh A. V., Ferri M., Tamplenizza M., Borghi F., Divitini G., Ducati C., Lenardi C., Piazzoni C., Merlini M., Podestà A., Milani P., *Nanotechnology*., 30 (2012) 475101.
21. Hassan S., Singh A. V., *J Nanosci Nanotechnol*., 9 (2014) 402.
22. Singh A. V., Galluzzi, M., Borghi F., Indrieri M., Vyas V., Podestà A., Gade W. N., *J. Nanosci Nanotechnol*., 13(2013)77.
23. Singh A. V., Batuwangala M., Mundra R., Mehta K., Patke S., Falletta E., Patil R., Gade W. N., *ACS Appl Mater Interfaces*.., 16 (2014) 14679.
24. Aitenneite, H., Abboud, Y., Tanane, O., Solhy, A., Sebti, S., Bouari, A. E., *J. Mater. Environ. Sci.* 7 (7) (2016) 2335.
25. Parab, H., Shenoy, N., Kumar, S. A., Kumar, S. D., Reddy, A.V.R., *J. Mater. Environ. Sci.* 7 (2016) 2468.
26. Uddin I., Adyanthaya, S., Syed A., Selvaraj K., Ahmad A., Poddar P., *J. Nanosci. Nanotechnol.* 8 (2008) 3909.
27. The XRD patterns were indexed with reference to the crystal structures from the PCPDFWIN: ZrO_2 (# 37-1484).
28. Murdie H. F., Morris M., Evans E., Paretzkin B., Wong-Ng W., Hubbard C. R., *Powder Diffr.* 1 (1986) 265.
29. Khan S. A., Gambhir S., Ahmad, A., *Beilstein J. Nanotechnol.* 5 (2014) 249.
30. Wagner C. D., *J. Vac. Sci. Technol.* 15 (1978) 518.
31. Margalit R., Vasquez R. P., *J. Protein. Chem*. 9 (1990) 105.
32. Nguyen T. D., Mrabet D., Vu T. T. D., Dinh C. T., Do T., *Cryst. Eng. Comm*. 13 (2011) 1450.
33. Moulder, J. F., Stickle, W. F., Sobol, P. E., Bomben, D., *Handbook of X-ray Photoelectron Spectroscopy*; Physics Electronics Int.: Eden Prairie, MN, 1995.
34. Bansal V., Rautaray D., Ahmad A., Sastry M., *J. Mater Chem*. 14 (2004) 3303.
35. Uddin, I., Poddar, P., Phogat, N., *Mater. Focus*., 2 (2013) 80.
36. Uddin I., Poddar P., Ahmad A., *J. Nanoeng. Nanomanuf*., 3 (2013) 91.
37. Antoine, R., Dugourd, P., *Phys. Chem. Chem. Phys*., 13 (2011) 16494.
38. Emeline A., Kataeva G. V., Litke, A. S., Rudakova A. V., Ryabchuk, V. K., Serpone N., *Langmuir* 14 (1998) 5011.